Published in final edited form as:
Transplant Proc. 2011 November ; 43(9): 3256–3261. doi:10.1016/j.transproceed.2011.10.031.

Cellular Immunoisolation for Islet Transplantation by a Novel Dual Porosity Electrospun Membrane

L. Krishnan, **L.R. Clayton**, **E.D. Boland**, **R.M. Reed**, **J.B. Hoying**, and **S.K. Williams**
Cardiovascular Innovation Insititute, Louisville, Kentucky, USA

Abstract

Immunoisolation strategies have the potential to impact the treatment of several diseases, such as hemophilia, Parkinson's and endocrine disorders, such as parathryroid disorders and diabetes. The hallmark of these disease states is the amelioration of the disease process by replacement of the deficient protein. Naturally, several cellular therapeutic strategies like genetically modified host cells, stem cells, donor cells, or even complex tissues like pancreatic islets have been investigated. Current evidence suggests that successful strategies must incorporate considerations for local hypoxia, vascularity, and immunoisolation. Additional regulatory concerns also include safe localization of implanted therapeutic cells to allow for monitoring, dose adjustment, or removal when indicated. Local hypoxia and cellular toxicity can be detrimental to the survival of freshly implanted pancreatic islets, leading to a need for a larger initial number of islets or repeated implantation procedures. The lack of adequate donors and the large number of islet equivalents needed to achieve euglycemic states amplify the nature of this problem. We have developed a novel immunoisolation device based on electrospun nylon, primarily for islet transplantation, such that the inner component functions as a cellular barrier while allowing diffusion, whereas the outer component can be optimized for tissue integration and accelerated vascularization. Devices explanted after subcutaneous implantation in wild-type B6 mice after a period of 30 days show vascular elements in the outer layer of the electrospun device. The inner layer when intact functioned as an effective barrier to cellular infiltration. The preimplantation of such a device, with a relatively thin inner barrier membrane, will allow for adequate vascularization and reduce postimplantation hypoxia. This study demonstrates the feasibility of an electrospun isolation device that can be easily assembled, modified by varying the electrospinning parameters, and functionalized with surface-active molecules to accelerate vascularization.

Almost 6% of the developed world's population has diabetes, a metabolic disorder of insulin deficiency and consequent hyperglycemia.[1] Traditional therapeutic management consists chiefly of restoring the metabolic homeostasis with exogenous insulin. About 10% of the Type 1 Diabetes Mellitus population is extremely sensitive to insulin and may lack proper glucagon response or other countermeasures and are at severe risk of hypoglycemia.[1] Additionally, about a third of Type 1 diabetics suffer from severe hypoglycemic episodes.[2] The goal of whole organ or purified islet transplantation is to produce a sustainable, exogenous insulin-independent euglycemic state. Beta cell replacement by free islet transplantation is an attractive alternative to conventional insulin replacement therapy,

Address reprint requests to Stuart K. Williams, PhD, Cardiovascular Innovation Institute, 302 East Muhammad Ali Boulevard, Room 105, Louisville, KY 40202, USA, stu.williams@louisville.edu.

especially in cases with poor glycemic control[3–5] However, problems such as high initial islet requirements (10^6 islets average) and need for secondary islet implants,[6] immunosuppression, rapid loss of islet cell mass, and shortage of donors or viable xenotransplantation alternatives limit its utility as a routine therapeutic intervention.[7] Emerging alternatives to portal delivery of islets (and risk of instant blood-mediated inflammatory reaction), such as direct implants at compatible sites, macro- or micro-encapsulation, or immunoisolation devices, have their own limitations. Hypoxic and diffusion-limited environments and loss of cell-cell or cell-extracellular matrix contacts can destabilize the islets and trigger apoptosis.[8] Our goal is to develop a nonbiodegradable, electrospun, prevascularized, subcutaneous cell delivery vehicle to support implantation of pancreatic islets. The device currently proposed is based on the dual porosity immunoisolation and vascularization layers proposed by Brauker et al.[9] The core concept of this device is that sequestration of implanted cellular elements within a defined physical constraint preventing antigenic elements, such as cell membrane debris from moving across into the host to elicit a humoral rejection response, while at the same timeallowing for efficient solute exchange (insulin, glucose, oxygen, and nutrients), will provide an ideal environment to isolate allogeneic islet cell transplants for therapy.

Several immunoisolation techniques are currently avilable and revolve around micro-or micro- encapsulation of islets in polymeric substrates[10,11] Although it is suggested that such membranes with porosities of 15–20 nm can be effective in immunoisolation,[12] it is also shown that they may not efficiently fractionate solutes based on their size in a diffusion-controlled environment driven by differences in concentration gradient, especially in the presence of a three-dimensional matrix on either side of the semipermeable membrane.[13] Furthermore, the convective water that fluxes through these small porosity membranes could be very low,[14] as in dialysis membranes, giving rise to concerns of effective cross-talk between blood glucose levels and amount of insulin released. Significanlty, Scharp et al[15] demonstrated that islets implanted in a hollow fiber membrane could remain viable and functional after short implantation in nonimmunosupressed hosts. But problems with most polymeric implants are the formation of a fibrous capsule, which over time can become relatively avascular, and the immediate postimplantation hypoxic environment. Electrospun polymers offer an ideal stategy to achieve this immunoisolation and provascularization role. The distinct advantage of this technology is the ability to control fiber and pore structures more accurately, within a thin membrane, and generate a more tortuous diffusion path for solutes than simple porous membrances as described im MEMS (micro electromechanical systems)-based immunoisolation strategies.[11] The ability to tailor the porosity of adjoining layers to allow vascular infiltration and the ease of functionalizing these polymers for linking surface active molecules or peptides are also seen as critical advantages in developing functional immunoisolation devices.

Materials and Methods

Assembly of Electrospun Device

Nylon pellets (Sigma Aldrich, St. Louis, Mo, United States) were dissolved in formic acid to obtain 15% and 40% solutions of nylon by weight. Pyridine was added to improve solution conductivity. The enclosed electrospinning chamber, with a rotating aluminum mandrel within it mounted on a translating platform, was electrically isolated. A syringe pump disepensed the polymer solution at a controlled rate through an 18-G needle tip. The needle tip was attached to a power supply providing +25 kV direct current (DC), thus creating a potential difference with respect to the rotating mandrel, which was connected to the electrical ground (Fig 1A). Fiber diameter, pore size, and thickness were controlled by varying the concentration of nylon, the dispensation rate, the distance between the spinning mandrel and the dispensing tip, and the volume of solution dispensed. Optimized spinning

parameters were used to first generate a tight mesh with small fiber diameter fibers using 15% nylon and subsequently this layer was immediately covered with a more porous second layer with larger fibrill diameters generated from electospinning of 40% nylon (Fig 1A–D). This dual porosity electrospun mat was then cut off the mandrel and stored under dehumidified conditions until further use. Two circular mat pieces were cut using a circular tissue punch and glued along the periphery (circumference) with the fine low-porosity layer facing inside. A polyethylene tube (Clay Adams, Division of Becton Dickinson, Parsippany, NJ, United States) was inserted across the circumferential edges into this pouch to form the only inlet into the device (Fig 2A). The devices were allowed to cure and then were sterilized in ethanol before implantation. A separate membrane was used to generate samples for scanning electron microscopy.

In Vivo Device Testing

Two wild-type black-6 strain mice were implanted with 2 devices each in the dorsal left and right subcutaneous space (haunches) under IACUC (institutional animal care and use committee) approval from the University of Louisville. The polyethylene delivery tube was trimmed, heat sealed, and interiorized in 1 mouse and exteriorized in the other to simulate both preloading and postloading of cells. When exteriorized, an anchoring suture around the tube stabilized the device inaddition to the staples sealing the skin incision. The animals were individually housed and were euthanized after 30 days to retrieve the devices.

Explant Immunohistochemistry

Explants were fixed in 4% paraformaldehyde and embedded into paraffin for sectioning. Serial sections, 6-μm thick, were taken from each of the 4 explanted devices and were stained with hematoxylin-easin (HE) and with Masson's trichrome (Fig 2B–E). Further sections were deparaffinized and stained with rhodamine-conjugated (Griffonia Simplicifolia lectin-1 (GS1; Vector Labs, Burlingame, Calif, United States) to label vasculature, antibody against smooth muscle alpha actin (a-SMC), and with DAPI (4′,6-diamidino-2-phenylindole) to identify cell nuclei. Fluorescently labeled specimens were imaged at the 3 different wavelengths (red, vessels; green, SMC; blue, nuclei) with a 20× air objective (Fig 2F). Three random areas each were imaged for at least to 2 to 3 sections of each device to generate a total of 31 distinct image sets (1 set, bright field; red, GS1; green, SMC; blue, nuclei).

Immunohistochemistry and Quantification of Vascularity

All image quantification procedures were performed in Metamorph (Molecular Devices, Downingtown, Penn, United States). Brightfield images were used for image calibration and to measure the thickness of the dual layered pouch at 2-distinct points per field of view (FOV; 20×). The nylon fibers are naturally fluorescent at the wavelengths examined. Hence, GS1- positive structures were manually identified from individual images of the redchannel (rhodamine). Ellipsoid regions of GS1-positive structures were duly marked with an ellipse that best fit the individual structure dimensions. In a few cases a clear lumen was not identifiable (vessels sectioned along axis rather than along diameters) and the brightest area at the ends of these structures were similarly marked with an ellipsoid. These ellipse regions were then overlaid on the a-SMC-positive areas to identify the vascular structures that also showed actin, representing an arteriole. The line and ellipse regions were exported for further analysis. The area of the ellipse was used to calculate the equivalent diameter of a circle and designated as the vessel diameter. Further more the total number of vessels and the percent age of arterioles were also estimated per FOV. A total of 31 image sets were analyzed for the 4 explants from the 2 mice.

Quantification of Physical Properties of Electrospun Membrane

Electrospun dual porosity mats were laid with either the inner or outer surface exposed, sputter coated with gold, and imaged on a scanning electron microscope (SEM, JEOL, Tokyo, Japan). Scanning electron microscope micrographs were acquired at appropriate magnifications for the inner and outer layer to enable clear visualization of the fibril and pore structure (Fig 1C and 1D). The micrographs were then imported into Metamorph (Molecular Devices, Sunnyvale, Calif, United States) and line elements were drawn to measure fibril diameters while elliptical elements were drawn to measure void areas such that the ellipse edges touched the crossing fibers (essentially the prolate that could fit through the void as seen in a two-dimensional plane). Twenty such random line and ellipsoids each were examined per representative micrograph of the inner and outer layers (n = 1 each). One image of each coponent was examined in this equantification. The area of the ellipsoids was converted to a representative diameter of an equivalent circle for clarity.

Results

The primary finding of this study is the ability of the dual-porosity electrospun nylon membrane to provide an effective barrier to cellular infiltration while supporting extensive tissue integration at the same time. Devices explanted from subcutaneous space of wild-type B6 mice did not show a significant tissue fibrotic response around them (Fig 2A). HE-stained sections of the explanted devices revealed high incorporation of cells in the membrane wall, especially in the outer porous area (Fig 2B). Blood vessels could be identified in the walls of the device demonstrating its ability to support vascularization even in the absence of a secondary pro-angiogenic surface modification or growth factors (Fig 2C and 2D). Significantly, the cellular infiltration was confined to the outer prorous section while the inner low-porosity layer was a barrier to infiltration when intact (Fig 2C, 2D, and 2E), arguing against the possibility that cell processes penetrate between the flexible fibers, gradually dislocating them, and finally moving through them into the device lumen. Masson's trichrome staining (Fig 2E), which showed pink tissue material in the inner membrane, but was still bound within it away from the lumen, confirms this belief. However, on occasion there are scattered cells seen on the luminal side of the device (Fig 2D), suggesting that the cells have migrated along this surface after an initial breach at a distant location. The integrity of the inner layer in this section, the high degree of infiltration in the porous layer along with the understanding that the process of membrane manipulation into this device could potentially cause microscale abrasions, especially of the thin inner component, leading to such a scenario.

The vascularization of these isolation membranes was confirmed by staining sections of the explant with GS1 (Griffonia Simplicifolia 1 - Lectin) for vascular endothelium, smooth muscle cells, and nuclei as shown in a composite image of a section in Fig 2F. Counting the number of GS1-positive structures incorporated in the explanted device showed an average of 9.48 (±0.64 SEM) vessels per field, as examined in 20× images. Also, 12.71% (±2.23 SEM) of these were found to be actin-positive arterioles. The average diameter of the vessel-like structures was 13.21 μm (±0.28 SEM). The average thickness of the electrospun membrane as measured from tissue sections was 99.24 μm (±0.86 SEM), which is close to the diffusion limit, but this includes the thickness of the outer porous layer, which in itself is vascularized. The large number of vessels per FOV of the sectioned membrane reinforces our design hypothesis that the high porosity outer component would provide support for neovascularization.

The inner component of the membrane with average pore size of 0.302 μm (±0.052 SD) and fiber diameter of 0.127 μm (±0.011 SEM) clearly serves as a thin and efficient cellular isolation barrier that will not impede solute transfer. Further more, the outer component of

this electrospun membrane with average pore size of 1.658 μm (±0.251 SD) and fiber diameter of 0.634 μm (±0.034 SEM) provides ample opportunity for tissue integration and vascularization.

Discussion

This study has established the proof of principle of an electrospun dual porosity membrane as an effective cellular isolation device. The porosity estimated by our study, although not inclusive of the tortuosity, clearly demonstrates a nanometer scale porous structure composed of thinner fibrils in the inner layer of this device. This size is orders of magnitude larger than proteins and solutes involved in cellular metabolism. Furthermore, given this porosity range of about 0.3 μm, it is understood that antibodies and complement system proteins will get across unhindered. Recent literature evidence based on MEMS technology further suggests that even pore sizes in the range of 20 nm may be insufficient to completely prevent complement proteins across such immunoisolation barriers.[12] Dionne et al[14] have, however, also demonstrated that absolute rejection of antibodies and complement proteins may not be critical for immunoisolative filters. The pore size in the device under study will, however, be an efficient barrier to destruction by T cells and macrophages. The current impact of this device is clearly in an autograft or allogeneic role where this cellular isolation device can provide all the benefits of cell transplantation while providing a safe localization of these therapeutic cells, both for dose adjustments and for manipulations in the face of adverse reactions. The development of complement quenching technologies [16,17] will provide future avenues for modification of this device for complete immunoisolation. Based on litetrature evidence, we believe that the porosity of the outer component is critical in both avoiding a massive fibrotic encapsulation response as well as in its provascularization role. ePTFE grafts with intermodal distance of 60 μm were conducive to microvascular invasion[18–20] but porosities in the range of 0.22 μm are not permissive to cellular infiltration.[21] The infiltration of our porous layer with GS1 + vessels could be due to the larger tortuosity and apparent larger pores than the ones estimated from two-dimensional images. The rapidity and degree of vascularization of this polymeric isolation device, along with the lack of formation of a thick fibrous capsule, and the demonstrated function of the inner layer as a barrier to cell infiltration render this isolation device as an ideal platform for the delivery of pancreatic islets. It is envisaged that delivery of pancreatic islets within this isolation device, which has already been prevascularized by subcutaneous implantation, will prevent islet death from ischemia immediately following delivery. Furthermore, the ease of manufacture, quality control, and implantation or retrieval of these electrospun isolation devices in the subcutaneous space make it viable for adjusting the critical dose of islet mass for independence from exogenous insulin. The isolation from the host cellular immune response and macro-phages and the reduced exposure load of implanted cell material to antigen-presenting systems are proposed to increase islet survival. We are currently evaluating this hypothesis in a diabetic mouse model.

Acknowledgments

Supported by funding from the National Institutes of Health RO1 DK078175 and EB077683.

References

1. Merani S, Shapiro AM. Current status of pancreatic islet transplantation. Clin Sci (Lond). 2006; 110:611. [PubMed: 16689680]
2. Leese GP, Wang J, Broomhall J, et al. Frequency of severe hypoglycemia requiring emergency treatment in type 1 and type 2 diabetes: a population-based study of health service resource use. Diabetes Care. 2003; 26:1176. [PubMed: 12663593]

3. Ryan EA, Lakey JR, Rajotte RV, et al. Clinical outcomes and insulin secretion after islet transplantation with the Edmonton protocol. Diabetes. 2001; 50:710. [PubMed: 11289033]
4. Marzorati S, Pileggi A, Ricordi C. Allogeneic islet transplantation. Expert Opin Biol Ther. 2007; 7:1627. [PubMed: 17961088]
5. Guyton, AC. Textbook of Medical Physiology. 8. W. B. Saunders Company; 1991.
6. Markmann JF, Deng S, Huang X, et al. Insulin independence following isolated islet transplantation and single islet infusions. Ann Surg. 2003; 237:741. [PubMed: 12796569]
7. Contreras JL. Extrahepatic transplant sites for islet xenotransplantation. Xenotransplantation. 2008; 15:99. [PubMed: 18447878]
8. Pinkse GG, Bouwman WP, Jiawan-Lalai R, et al. Integrin signaling via RGD peptides and anti-beta1 antibodies confers resistance to apoptosis in islets of Langerhans. Diabetes. 2006; 55:312. [PubMed: 16443762]
9. Brauker JH, Carr-Brendel VE, Martinson LA, et al. Neovas-cularization of synthetic membranes directed by mebrane microarchitecture. J Biomed Mater Res. 1995; 29:1517. [PubMed: 8600142]
10. Gimi B, Kwon J, Kuznetsov A, et al. A nonoporous, transparent microcontainer for encapsulated islet therapy. J Diabetes Sci Technol. 2009; 3:297. [PubMed: 19746206]
11. Desai TA, West T, Cohen M, et al. Nanoporous microsystems for islet cell replacement. Adv Drug Deliv Rev. 2004; 56:1661. [PubMed: 15350295]
12. Desai TA, Hansford DJ, Chu WH, et al. Investigating islet immunoisolation parameters using microfabricated membranes. Materials Research Society Symposium Proceedings. 1998; 530:7.
13. Iwata H, Morikawa N, Ikada Y. Permeability of filters used for immunoisolation. Tissue Eng. 1996; 2:289. [PubMed: 19877960]
14. Dionne KE, Cain BM, Li RH, et al. Transport characterization of membranes for immunoisolation. Biomaterials. 1996; 17:257. [PubMed: 8745322]
15. Scharp DW, Swanson CJ, Olack BJ, et al. Protection of encapsulated human islets implanted without immunosuppression in patients with type I or type II diabetes and in nondiabetic control subjects. Diabetes. 1994; 43:1167. [PubMed: 8070618]
16. Wang W, Gu Y, Hori H, et al. Subcutaneous transplantation of macroencapsulated porcine pancreatic endocrine cells normalizes hyperglycemia in diabetic mice. Transplantation. 2003; 76:290. [PubMed: 12883181]
17. Murakami Y, Iwata H, Kitano E, et al. Interaction of poly (styrene sulfonic acid) with the alternative pathway of the serum complement system. J Biomater Sci Polym Ed. 2005; 16:381. [PubMed: 15850291]
18. Clowes AW, Kirkman TR, Reidy MA. Mechanisms of arterial graft healing. Rapid transmural capillary ingrowth provides a source of intimal endothelium and smooth muscle in porous PTFE prostheses. Am J Pathol. 1986; 123:220. [PubMed: 3706490]
19. Clowes AW, Zacharias RK, Kirkman TR. Early endothelial coverage of synthetic arterial grafts: porosity revisited. Am J Surg. 1987; 153:501. [PubMed: 2953265]
20. Sharkawy AA, Klitzman B, Truskey GA, et al. Engineering the tissue which encapsulates subcutaneous implants. II. Plasma-tissue exchange properties. J Biomed Mater Res. 1998; 40:586. [PubMed: 9599035]
21. Padera RF, Colton CK. Time course of membrane microarchitecture-driven neovascularization. Biomaterials. 1996; 17:277. [PubMed: 8745324]

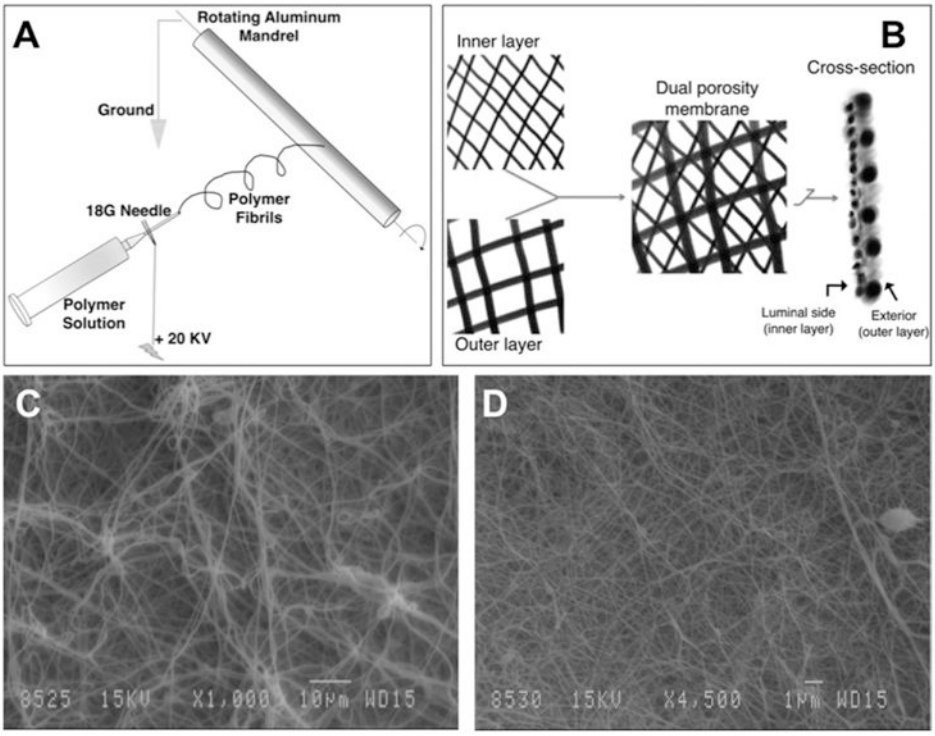

Fig 1.

(**A**) Schematic demonstrating the electrospinning procedure. The system beyond the tip of the 18-G needle is electrically isolated to allow fiber deposition on the rotating mandrel. (**B**) Schematic of the dual porosity immunoisolation membrane. The 15% nylon is first spun on the rapidly rotating mandrel followed immediately by the 40% nylon on the now slowly spinning and rapidly transplating mandrel. The cross- section schematic demonstrates the configuration in which the membrane is glued together to form a pouch. Two such mats are glued at the edges such that the inner nylon layer faces the luminal aspect. (**C**) Scanning electron microscope micrograph (original magnification, 1000×) showing larger fibrils and pores of the outer layer. (**D**) Scanning electron microscope micrograph (original magnification, 4500×) showing fine fibers and pores of the immunoisolating inner layer.

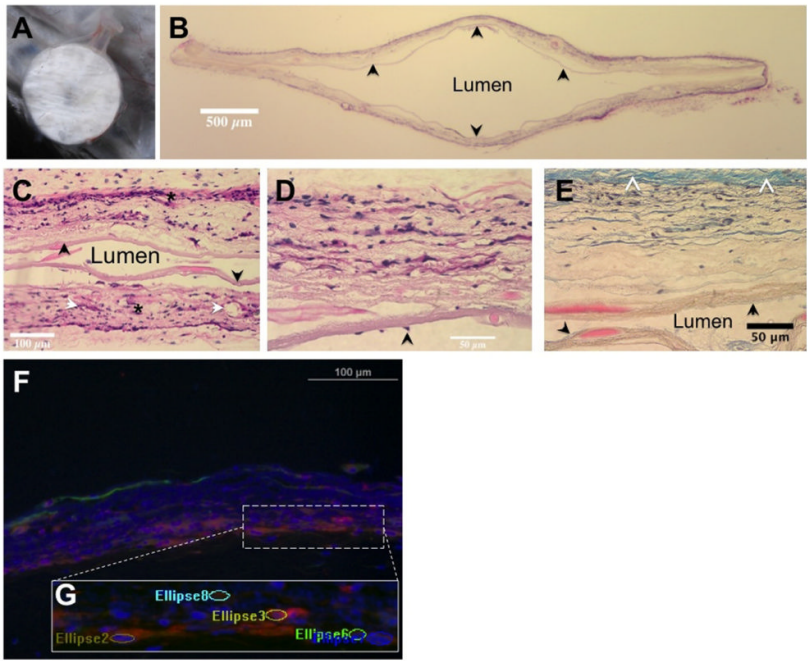

Fig 2.

(**A**) Subcutaneously implanted immunoisolation device at time of explant. Note the vascularity and lack of large fibrotic response. (**B**) (H&E) stained transverse section of a device (original magnification, 1×). The central lumen is cell-free, the outer layer shows significant cellular infiltration. The inner layer (arrow) is intact through the cross-section. (**C**) H&E stained image of the central luminal area clearly shows tissue integration of outer layers (*) on either side while the intact inner layers (arrow) serve as a barrier to cells moving across (original magnification, 20×). Also identified are some vascular elements (white arrows). (**D**) H&E section focused on a single wall of the device reinforces the tissue integrative and cellular barrier natures of the outer and inner layers, respectively (original magnification, 40×). Scattered cells on the luminal aspect (arrow) without apparent breach of inner layer may suggest migration of cells from an area of loss of integrity. (**E**) Section of the device wall stained with Masson's trichrome (original magnification, 40×). Note the relatively small amount of collagenous tissue capsule (white arrowheads). The inner (black arrow) and outer membranes are clearly demarcated, confirming the cellular penetration of only the outer layer of the device while the lumen is cell- free. (**F**) Composite image of immunostained sections showing vascular structures, smooth muscle cells, and cell nuclei. (**G**) The ellipsoid regions counted as vascular elements overlaid on a magnified area of the image.